NASA TECHNICAL MEMORANDUM

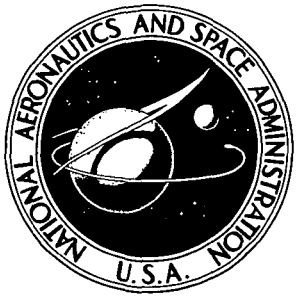

NASA TM X-2991

NASA TM X-2991

BUCKLING OF A CONICAL SHELL WITH LOCAL IMPERFECTIONS

by Paul A. Cooper and Cornelia B. Dexter

Langley Research Center
Hampton, Va. 23665

NATIONAL AERONAUTICS AND SPACE ADMINISTRATION • WASHINGTON, D. C. • JULY 1974

1. Report No.	2. Government Accession No.	3. Recipient's Catalog No.
NASA TM X-2991		

4. Title and Subtitle	5. Report Date
BUCKLING OF A CONICAL SHELL WITH LOCAL IMPERFECTIONS	July 1974
	6. Performing Organization Code

7. Author(s)	8. Performing Organization Report No.
Paul A. Cooper and Cornelia B. Dexter	L-9331
	10. Work Unit No.
9. Performing Organization Name and Address	743-32-11-01
NASA Langley Research Center Hampton, Va. 23665	11. Contract or Grant No.
	13. Type of Report and Period Covered
12. Sponsoring Agency Name and Address	Technical Memorandum
National Aeronautics and Space Administration Washington, D.C. 20546	14. Sponsoring Agency Code

15. Supplementary Notes

16. Abstract

Small geometric imperfections in thin-walled shell structures can cause large reductions in buckling strength. Most imperfections found in structures are neither axisymmetric nor have the shape of buckling modes but rather occur locally. This report presents the results of a study of the effect of local imperfections on the critical buckling load of a specific axially compressed thin-walled conical shell. The buckling calculations were performed by using a two-dimensional shell analysis program referred to as the STAGS (STructural Analysis of General Shells) computer code, which has no axisymmetry restrictions.

Results show that the buckling load found from a bifurcation buckling analysis is highly dependent on the circumferential arc length of the imperfection type studied. As the circumferential arc length of the imperfection is increased, a reduction of up to 50 percent of the critical load of the perfect shell can occur. The buckling load of the cone with an axisymmetric imperfection is nearly equal to the buckling load of imperfections which extended 60° or more around the circumference, but would give a highly conservative estimate of the buckling load of a shell with an imperfection of a more local nature.

17. Key Words (Suggested by Author(s))	18. Distribution Statement
Conical shell buckling Conical shell instability Shell imperfections	Unclassified – Unlimited STAR Category 32

19. Security Classif. (of this report)	20. Security Classif. (of this page)	21. No. of Pages	22. Price*
Unclassified	Unclassified	21	$3.00

*For sale by the National Technical Information Service, Springfield, Virginia 22151

BUCKLING OF A CONICAL SHELL WITH LOCAL IMPERFECTIONS

By Paul A. Cooper and Cornelia B. Dexter
Langley Research Center

SUMMARY

Small geometric imperfections in thin-walled shell structures can cause large reductions in buckling strength. Most imperfections found in structures are neither axisymmetric nor have the shape of buckling modes but rather occur locally. This report presents the results of a study of the effect of local imperfections on the critical buckling load of a specific axially compressed thin-walled conical shell. The buckling calculations were performed by using a two-dimensional shell analysis program referred to as the STAGS (STructural Analysis of General Shells) computer code, which has no axisymmetry restrictions.

Results show that the buckling load found from a bifurcation buckling analysis is highly dependent on the circumferential arc length of the imperfection type studied. As the circumferential arc length of the imperfection is increased, a reduction of up to 50 percent of the critical load of the perfect shell can occur. The buckling load of the cone with an axisymmetric imperfection is nearly equal to the buckling load of imperfections which extended 60° or more around the circumference, but would give a highly conservative estimate of the buckling load of a shell with an imperfection of a more local nature.

INTRODUCTION

Small geometric imperfections in thin-walled shell structures can cause large reductions in buckling strength. Much work has been done to establish the buckling imperfection sensitivity of shell-of-revolution structures containing small geometric imperfections either axisymmetric in shape or in the shape of classical buckling modes. (See, for example, refs. 1 to 3.) In practice, however, most imperfections found in structures are neither axisymmetric nor have the shape of buckling modes but rather occur locally. This report presents the results of a study of the effect of local imperfections on the critical buckling load of a specific axially compressed thin-walled conical shell. The study was motivated by a need to establish the degradation of the axial load carrying ability of a thin-walled conical portion of a fielded missile system which had sustained local damage during routine handling and shipping. The buckling calculations

were performed by using a two-dimensional shell analysis program referred to as the STAGS (STructural Analysis of General Shells) computer code (ref. 4), which has no axisymmetry restrictions.

SYMBOLS

E	Young's modulus
$m_{\bar{x}}$	multiple of thickness such that $m_{\bar{x}}t$ defines axial extent of imperfection
$n_{\bar{y}}$	one-half of multiple of thickness such that $2n_{\bar{y}}t$ defines lineal circumferential extent of imperfection
P_{cr}	critical axial buckling load
$\overline{P}_{cr}$	classical critical axial buckling load (see eq. (2))
R_o	nominal radius of cone at central location of imperfection
t	shell wall thickness
u	meridional displacement
v	circumferential displacement
w	normal displacement
w_{max}	maximum amplitude of buckled shell
W	normal measure of imperfection measured from nominal cone surface
W_{max}	maximum amplitude of imperfection
x	lineal axial distance measured from small radius end of cone
$\bar{x}$	local axial distance measured from the beginning of the imperfection
$\bar{y}$	angular circumferential distance measured from center of imperfection, rad

α semivertex angle of cone

β circumferential extent of imperfections, deg

θ coordinate in the circumferential direction measured from center of imperfection, deg

μ Poisson's ratio

ϕ meridional edge rotation

PROBLEM DEFINITION

Shell Geometry, Edge Condition, and Loading

The shell segment, with dimensions as shown in figure 1, is an idealization of an unstiffened aluminum truncated conical shell with stiff end rings. The end rings are assumed to be rigid in the end plane and, thus, are approximated by simply supported boundary conditions such that the normal displacement w and the circumferential displacement v are fixed. At the upper edge (small radius edge), the meridional displacement u and the edge rotation ϕ are free. At the lower edge, the edge rotation ϕ is also free but the in-plane displacement u is fixed to support the applied load. A uniform compressive meridional unit line load is applied at the small radius edge. Any normal load component which might occur in the actual missile system is assumed to be equilibrated by the stiff end ring idealization.

Imperfection Geometry

The imperfection sizes of immediate interest in this report have an axial extent of 50t, with a maximum inward depth normal to the surface of 5t and various circumferential lengths, where t is the shell wall thickness. The imperfection covers a portion of the shell bounded by two meridians and two parallel circles. The meridional center of the imperfection is located about two-thirds of the axial distance from the small radius edge of the cone (fig. 2(a)). In this study, the circumferential extent of the imperfection is varied from 0° to 180°. A highly localized imperfection (i.e., one contained within a small region of the shell) with a meridional length of 50t, circumferential arc length of 50t, and maximum normal amplitude of 5t was studied in detail, and results for this case are presented in a subsequent section. The imperfection is assumed to have a shape defined by

$$W = \frac{W_{max}}{2}\left[\left(\cos\frac{2\pi\bar{x}}{m\bar{x}t} - 1\right)\left(\cos\frac{\pi\bar{y}R_o}{2n\bar{y}t}\right)\right] \tag{1}$$

To make use of symmetry properties in the analysis, a diametrical plane of symmetry is assumed so that two imperfections centered 180^o apart are assumed to exist for all studies made in this report. For an extent of 180^o, the two diametrical imperfections meet.

ANALYSIS

All asymmetric imperfection calculations were performed with the STAGS computer code. The STAGS code uses a two-dimensional finite-difference scheme to approximate the shell energy equations which are minimized to obtain the stress distribution and/or stability of thin general shell structures. As shown in equation (1), the imperfection is formed by using the normal displacement only, and only the first partial derivatives of the imperfection function are used in the STAGS analysis. This method of representing the imperfection is an approximation to the accurate shell equations which would strictly define the imperfection and is probably accurate only for imperfections of shallow amplitudes (less than 10t). The STAGS code is capable of calculating either a nonlinear collapse load or a bifurcation buckling load away from a linear prebuckled state. In this study, only a bifurcation buckling analysis is performed and prebuckling rotations are not taken into account.

To perform the analysis most efficiently, only a 90^o portion of the shell (fig. 2(b)) was studied. Thus, symmetry conditions were enforced along the meridian at $\theta = 0^o$ and 90^o. In this study, the number of finite-difference stations along the meridian is 33 and the number of stations along one-fourth of the circumference is 51. A preliminary study showed that the grid size resulting from the use of this number of stations was sufficiently fine to give an accurate solution. This grid point network contains approximately 5000 degrees of freedom. The locations of the finite-difference stations along the meridian and along the circumference are shown in figures 2(a) and 2(b), respectively, for the imperfection with a circumferential extent of 50t. Regions of large stress gradients have a denser grid spacing. All analyses with the exception of the perfect cone (i.e., a cone with no imperfection) use the same number of degrees of freedom and same location of stations along the meridian. The number of stations along the circumference is the same for all problems, but the spacing of the stations is adjusted for each circumferential imperfection length investigated so that close spacing is attained in the region of the imperfection.

RESULTS AND DISCUSSION

The results are presented in two parts. First, the results for a series of imperfections of 50t axial length, 5t depth, and various circumferential lengths up to an included arc length of 180° are discussed and then results from an in-depth study of a local imperfection with a circumferential arc length of 50t are examined in detail.

Effect of Circumferential Extent of Imperfection

Figure 3 is a plot of the critical buckling ratio $P_{cr}/\overline{P}_{cr}$ as the circumferential arc length of the imperfections β is increased from 0° to 180°. The classical buckling load P_{cr} is approximated by the equivalent cylinder buckling formula

$$\overline{P}_{cr} = \frac{2\pi Et^2 \cos^2\alpha}{\sqrt{3(1 - \mu^2)}} \tag{2}$$

which is given in reference 5 and for the shell of figure 1 would be

$$\overline{P}_{cr} = 665.9 \text{ kN } (149\,700 \text{ lb})$$

For values of β less than 15°, there is essentially no change in buckling strength. For values of β from 15° to 70°, a rapid drop in buckling load is observed; whereas, for β values between 70° and 140°, the critical load remains nearly constant at about 55 percent of the critical load of the perfect cone. This behavior is similar to experimental and analytical results reported for cylindrical shells with cutouts (e.g., ref. 6). As the edges of the opposing imperfections approach each other, the critical load once again starts to drop and at $\beta = 180^{\circ}$, when the edges of the two imperfections begin to overlap, the buckling load has reduced to approximately 40 percent of the critical load of the perfect cone.

The buckling load of the cone with an axisymmetric imperfection defined by equation (1) with $\bar{y} = 0$ was determined by using a computer program for bifurcation buckling of shells of revolution about an axisymmetric prebuckling state (ref. 7). The buckling load is 54 percent of the critical load of the perfect cone and the cone buckles into eight circumferential waves. The buckling load is shown as a horizontal line in figure 3 for comparison purposes. The axisymmetric results give a fairly accurate prediction of the critical buckling load for imperfections which extend over 60° or more of included angle around the circumference, but the prediction is highly conservative for imperfections of more local nature. The axisymmetric imperfection results differ from the results for two diametrically opposed imperfections of 180° extent since the

amplitude of the latter imperfections varies sinusoidally in the circumferential direction, whereas the amplitude of the axisymmetric imperfection is constant.

Local Imperfection

The prebuckling and buckling results for the specific imperfection shown in figure 2(b) with a circumferential extent of 50t ($\beta = 10.5^{o}$) are now presented in more detail. As shown in figure 3, the buckling load for this imperfection is essentially the same as the classical buckling load for the perfect cone. The axial distribution of meridional prebuckling stress for the 50t circumferential imperfection is given in figure 4. For a cone with no imperfection, the meridional prebuckling stress varies linearly along the meridian. As indicated in figure 4(a), a meridional distribution at $\theta = 1^{o}$ shows a rapid reduction in compressive stress in the imperfection to essentially zero stress in the imperfection center. The stress variation along the meridian at $\theta = 38^{o}$ is presented in figure 4(b) and is seen to be nearly linear and to approximate nominal perfect shell behavior. Figure 4(c) shows the stress variation along a circumference taken near the lower edge of the imperfection. The stress is zero at the center of the imperfection ($\theta = 0^{o}$) with a peak in stress occurring at the edge of the imperfection. The stress then rapidly damps to the perfect shell value of -0.84 for a unit applied load and remains uniform from $\theta = 20^{o}$ to 90^{o}. This relatively large stress concentration at the edge of the imperfection is caused by a stress redistribution around the imperfection. Since the total axial load must be the same as the applied axial load at the top edge, the stress peak is expected since the center of the imperfection has zero stress. The maximum in-plane stress occurs at the meridional center of the imperfection just outside the circumferential edge of the imperfection (x = 54.8 cm (21.57 in.)) and is 1.56; this is a 56-percent increase over the maximum in-plane stress of the perfect shell.

Figures 5(a) and 5(b) show the normal displacement buckling mode normalized with respect to w_{max} along a circumference which cuts close to the center of the imperfection (x = 55.1 cm (21.7 in.)) and along a meridian which nearly cuts through the center of the imperfection ($\theta = 1^{o}$). The maximum displacement occurs in the vicinity of the imperfection. However, the buckling amplitudes do not damp appreciably and the instability may be classified as a general instability rather than a local instability.

The critical load with two diametrically opposed imperfections each of 90^{o} extent is 52 percent of the classical critical load. Figures 6 and 7 which show the prebuckling meridional stress resultant and normal displacement buckling mode, respectively, are included to demonstrate the difference in the behavior of the structure when the circumferential extent of the imperfection has been increased from a highly local extent to 90^{o}. A local stress rise occurs near the edge of the imperfection as shown in figure 6(a). This large stress rise can be contrasted with the slight stress increase along a meridian

at a location outside the imperfection ($\theta = 70^{\circ}$) as shown in figure 6(b). This stress distribution character along the circumference is illustrated in figure 6(c) where the effect on stress of the imperfection rapidly dissipates outside the imperfection. The local character of the buckling mode in the meridional direction as shown in figure 7(a) can be contrasted with the more global character of the buckling mode shown in figure 5(b) for the local imperfection. The more local character of the buckling mode along the circumference can be seen by comparing the modal behavior shown in figure 7(b) with that of figure 5(a). The buckling displacements remain local to the imperfection and damp rapidly away from the imperfection in both the meridional and circumferential directions.

CONCLUDING REMARKS

A brief study was made of the effect of a particular type of local imperfection on the buckling of an axially compressed thin-walled conical shell. Results show that the buckling load found from a bifurcation buckling analysis is highly dependent on the circumferential arc length of the imperfection type studied. As the circumferential arc length of the imperfection is increased, a reduction of up to 50 percent of the critical load of the perfect shell can occur. The buckling load of the cone with an axisymmetric imperfection is nearly equal to the buckling load of imperfections which extended 60° or more around the circumference, but would give a highly conservative estimate of the buckling load of a shell with an imperfection of a more local nature.

The bifurcation buckling analysis of a highly localized imperfection shows no significant drop in buckling load but the linear static stress analysis shows that the imperfection does cause a local stress rise of over 50 percent above the maximum stress in the perfect cone. For small imperfections the buckling mode can be classified as a general shell instability, but the buckled region tends to remain local to the imperfection as the imperfection size is increased circumferentially.

Langley Research Center,
National Aeronautics and Space Administration,
Hampton, Va., May 2, 1974.

REFERENCES

1. Stein, Manuel: Some Recent Advances in the Investigation of Shell Buckling. AIAA J., vol. 6, no. 12, Dec. 1968, pp. 2339-2345.

2. Amazigo, J. C.; and Budiansky, B.: Asymptotic Formulas for the Buckling Stresses of Axially Compressed Cylinders With Localized or Random Axisymmetric Imperfections. Trans. ASME, Ser. E: J. Appl. Mech., vol. 39, no. 1, Mar. 1972, pp. 179-184.

3. Narasimhan, K. Y.; and Hoff, N. J.: Snapping of Imperfect Thin-Walled Circular Cylindrical Shells of Finite Length. Trans. ASME, Ser. E: J. Appl. Mech., vol. 38, no. 1, Mar. 1971, pp. 162-171.

4. Almroth, B. O.; Brogan, F. A.; and Marlowe, M. B.: Collapse Analysis for Shells of General Shape. Volume I – Analysis. AFFDL-TR-71-8, U.S. Air Force, Aug. 1972.

5. Anon.: Buckling of Thin-Walled Truncated Cones. NASA SP-8019, 1968.

6. Starnes, James H., Jr.: Effect of a Circular Hole on the Buckling of Cylindrical Shells Loaded by Axial Compression. AIAA J., vol. 10, no. 11, Nov. 1972, pp. 1466-1472.

7. Cohen, Gerald A.: Computer Analysis of Ring-Stiffened Shells of Revolution. NASA CR-2085, 1973.

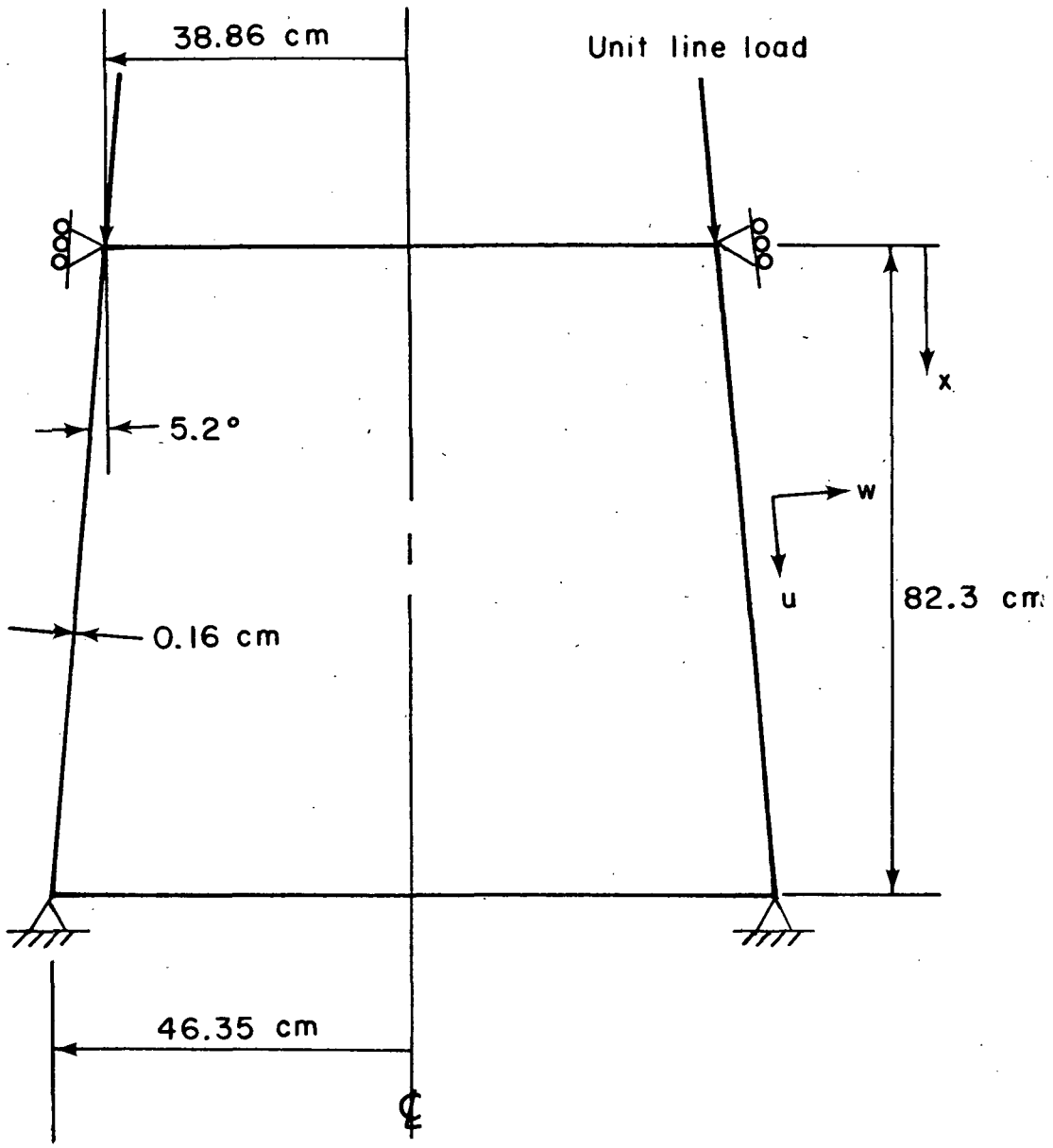

Figure 1.- Shell geometry.

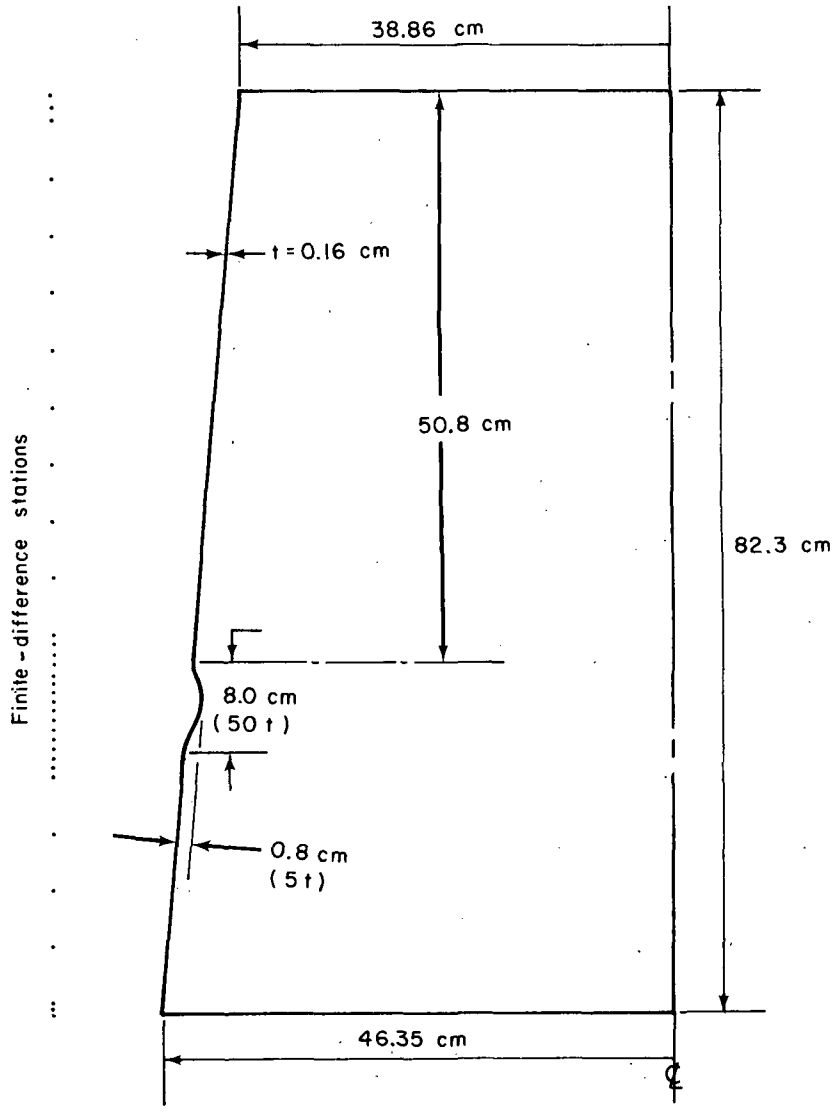

(a) Axial grid at $\theta = 0^{o}$.

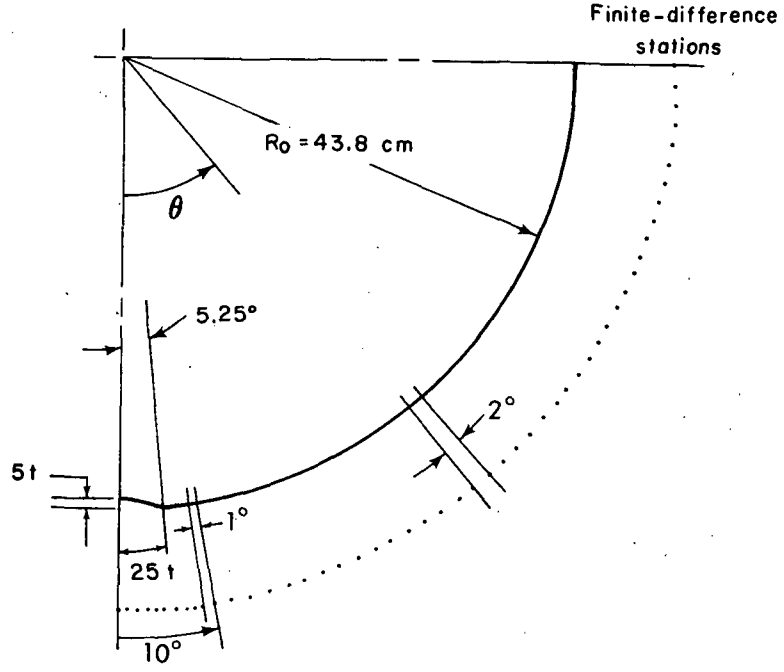

(b) Circumferential grid at x = 54.8 cm. t = 0.16 cm.

Figure 2.- Typical finite-difference representation.

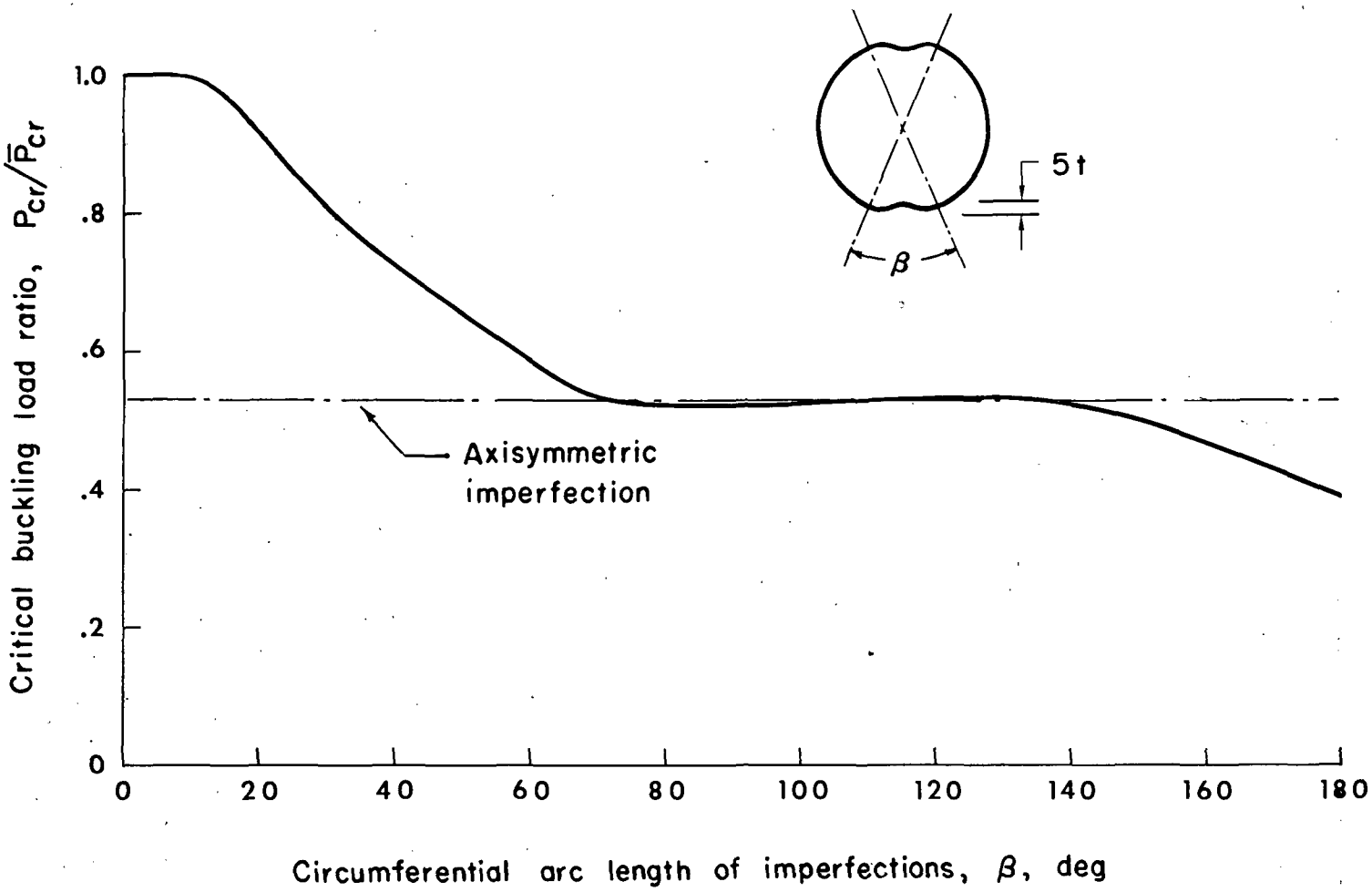

Figure 3.- Effect of the circumferential extent of local imperfection on the critical buckling load of a small-angle cone. $\bar{P}_{cr}$ = 665.9 kN.

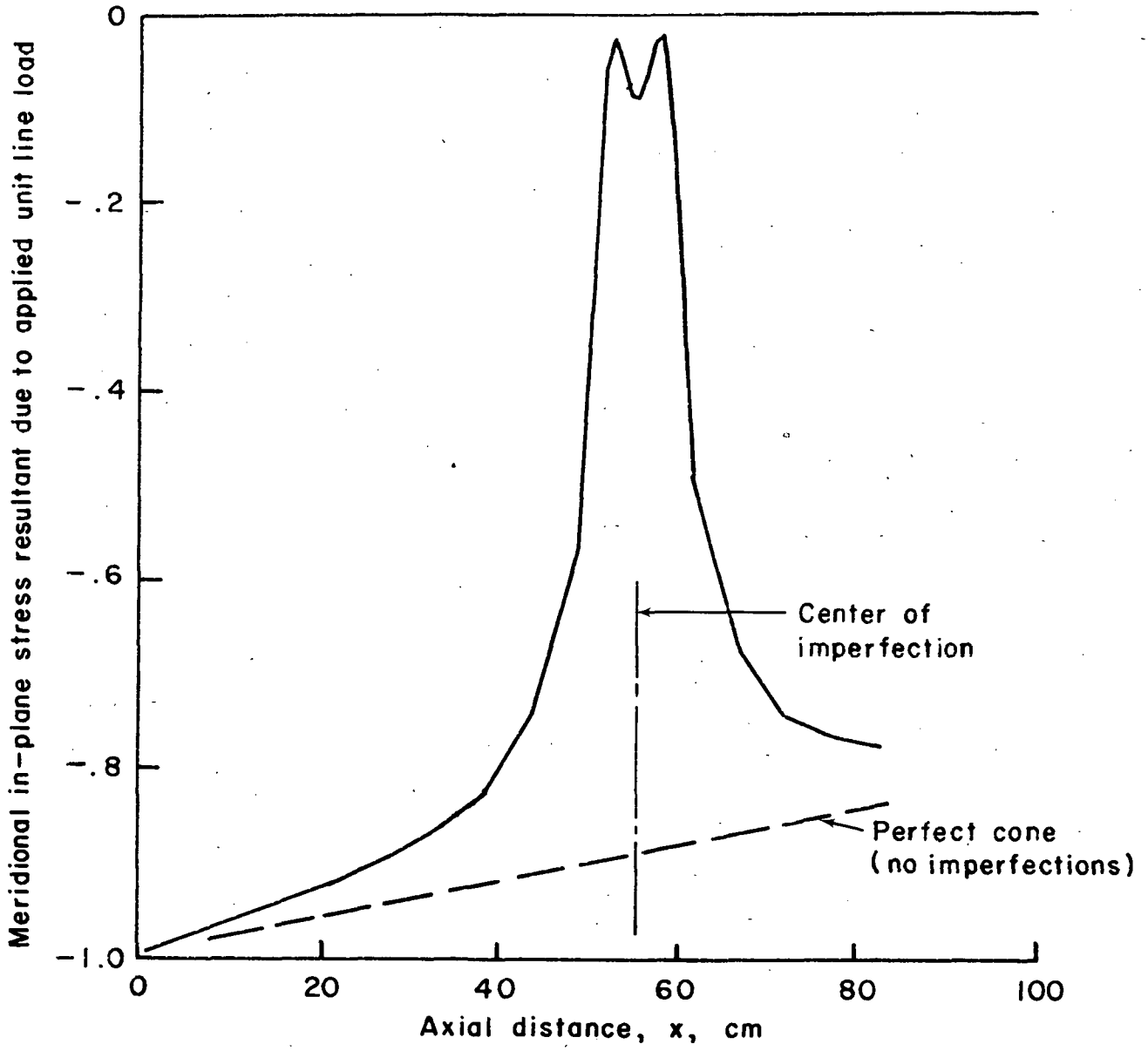

(a) $\theta = 1^{o}$ (near center of imperfection).

Figure 4.- Prebuckling meridional in-plane stress resultant distribution due to unit loading for a cone with highly localized imperfection. (Circumferential arc length of imperfection equals 50t.)

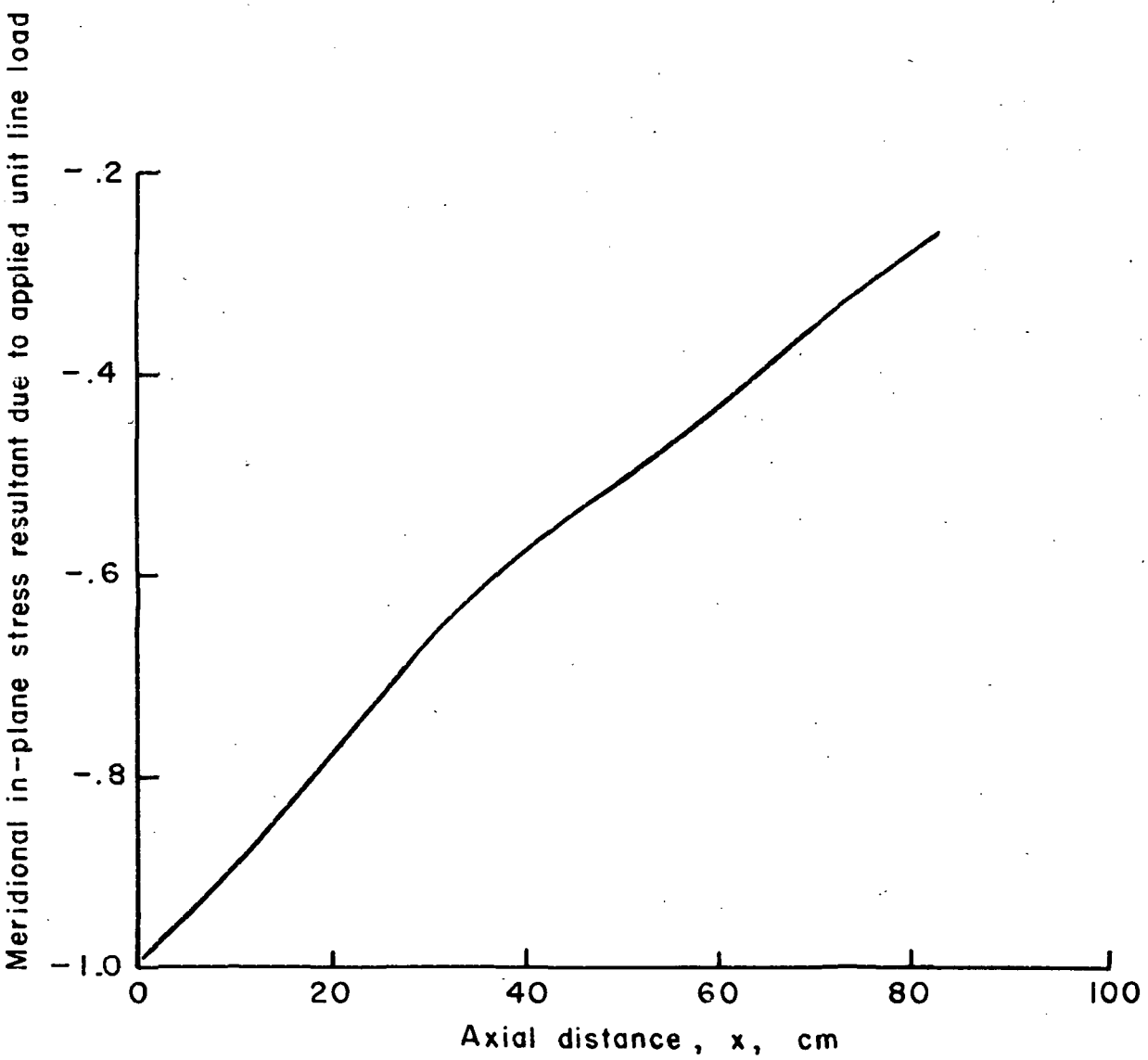

(b) $\theta = 38^{\circ}$.

Figure 4.- Continued.

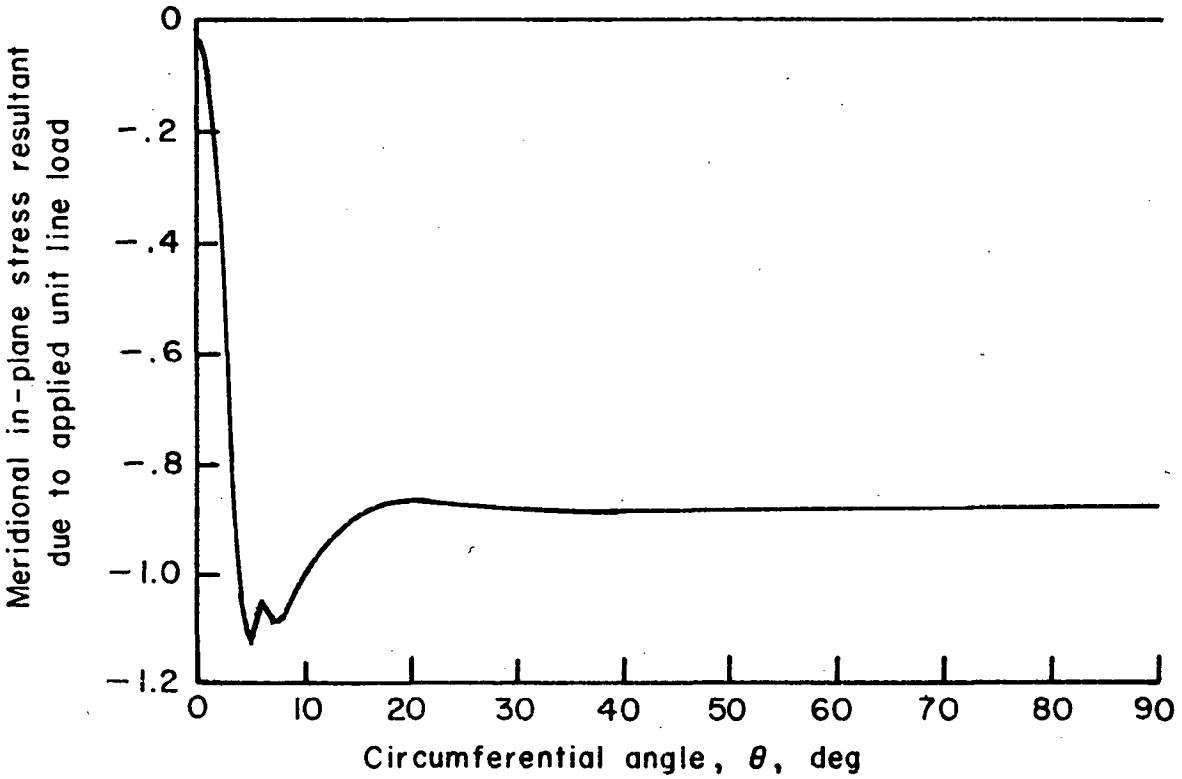

(c) x = 58.4 cm (lower edge of imperfection).

Figure 4.- Concluded.

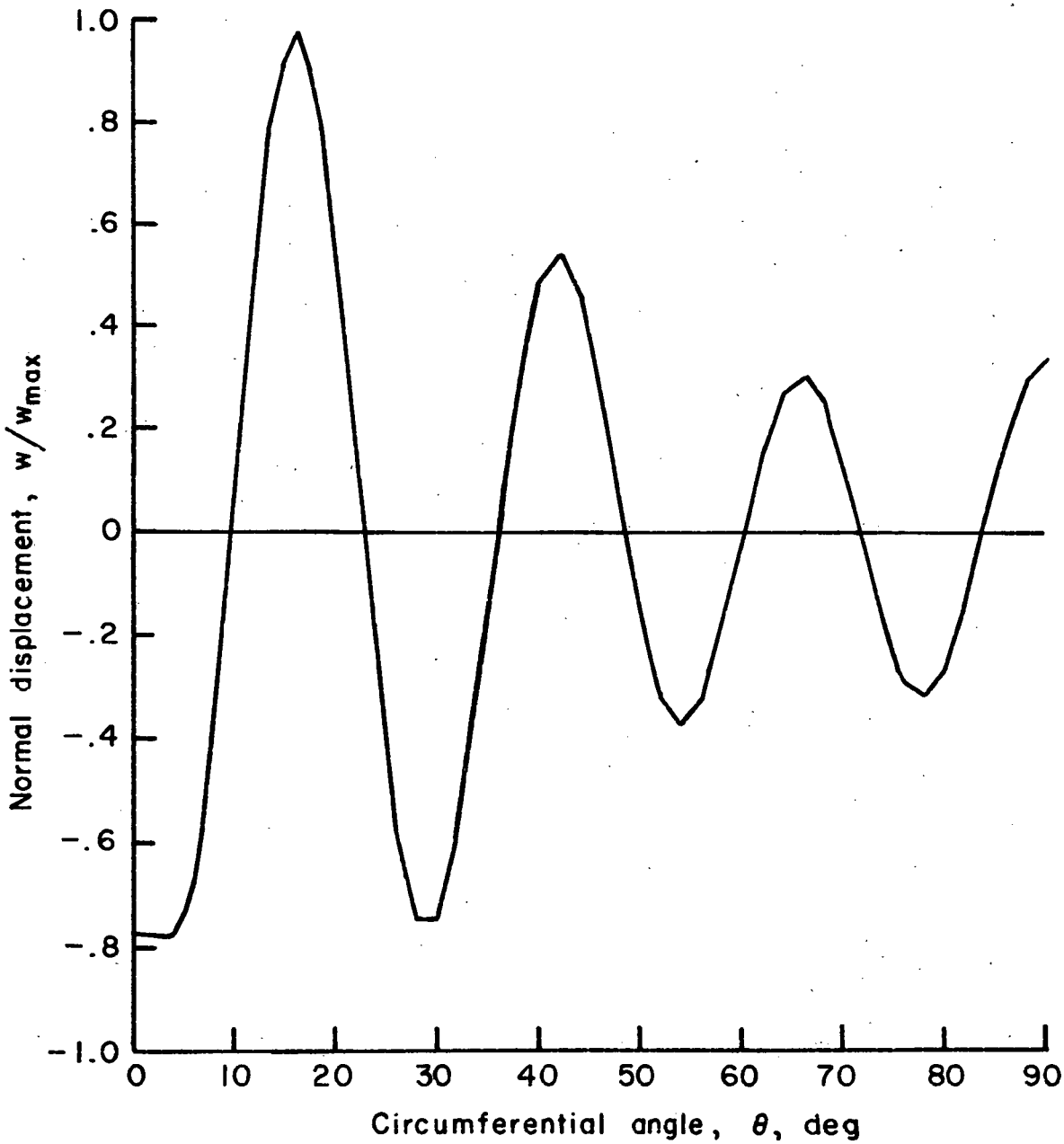

(a) x = 55.1 cm (near center of imperfection).

Figure 5.- Normal displacement buckling mode of a cone with highly localized imperfection. (Circumferential arc length of imperfection equals 50t.)

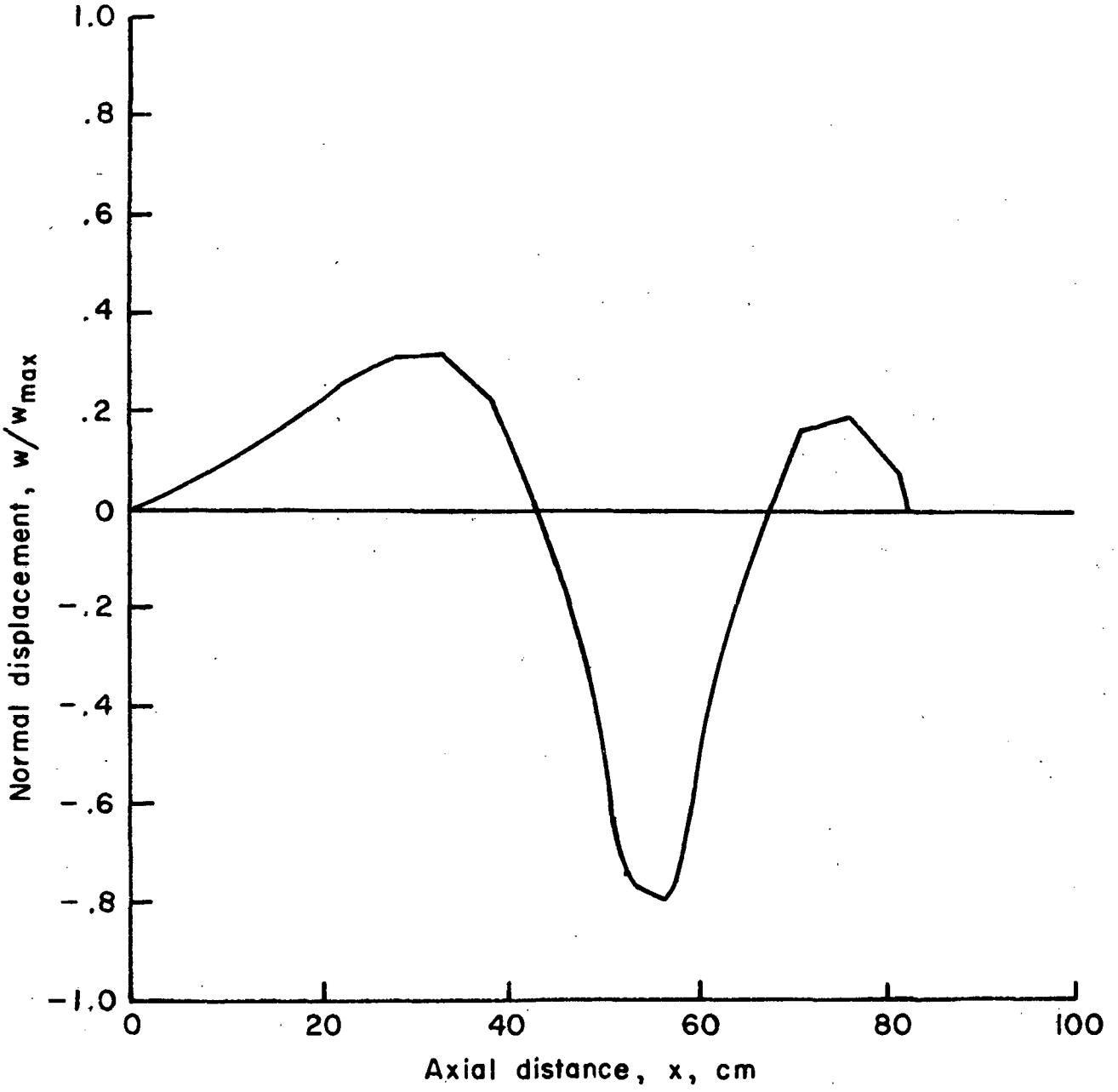

(b) $\theta = 1^{o}$ (near center of imperfection).

Figure 5.- Concluded.

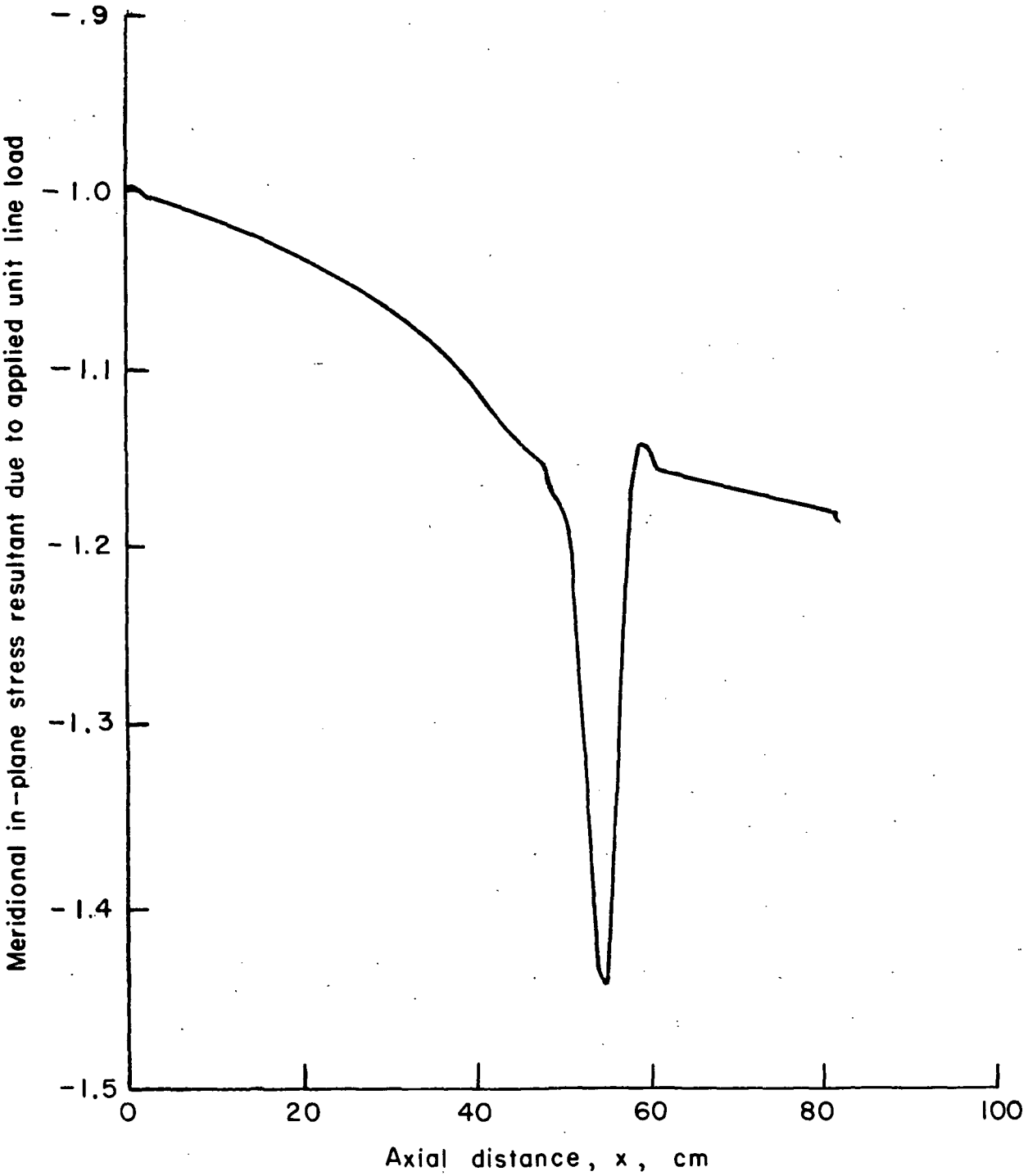

(a) $\theta = 41.1^{o}$ (near edge of imperfection).

Figure 6.- Prebuckling meridional in-plane stress resultant distribution due to unit loading for a cone with imperfection extending 90^{o} along the circumference.

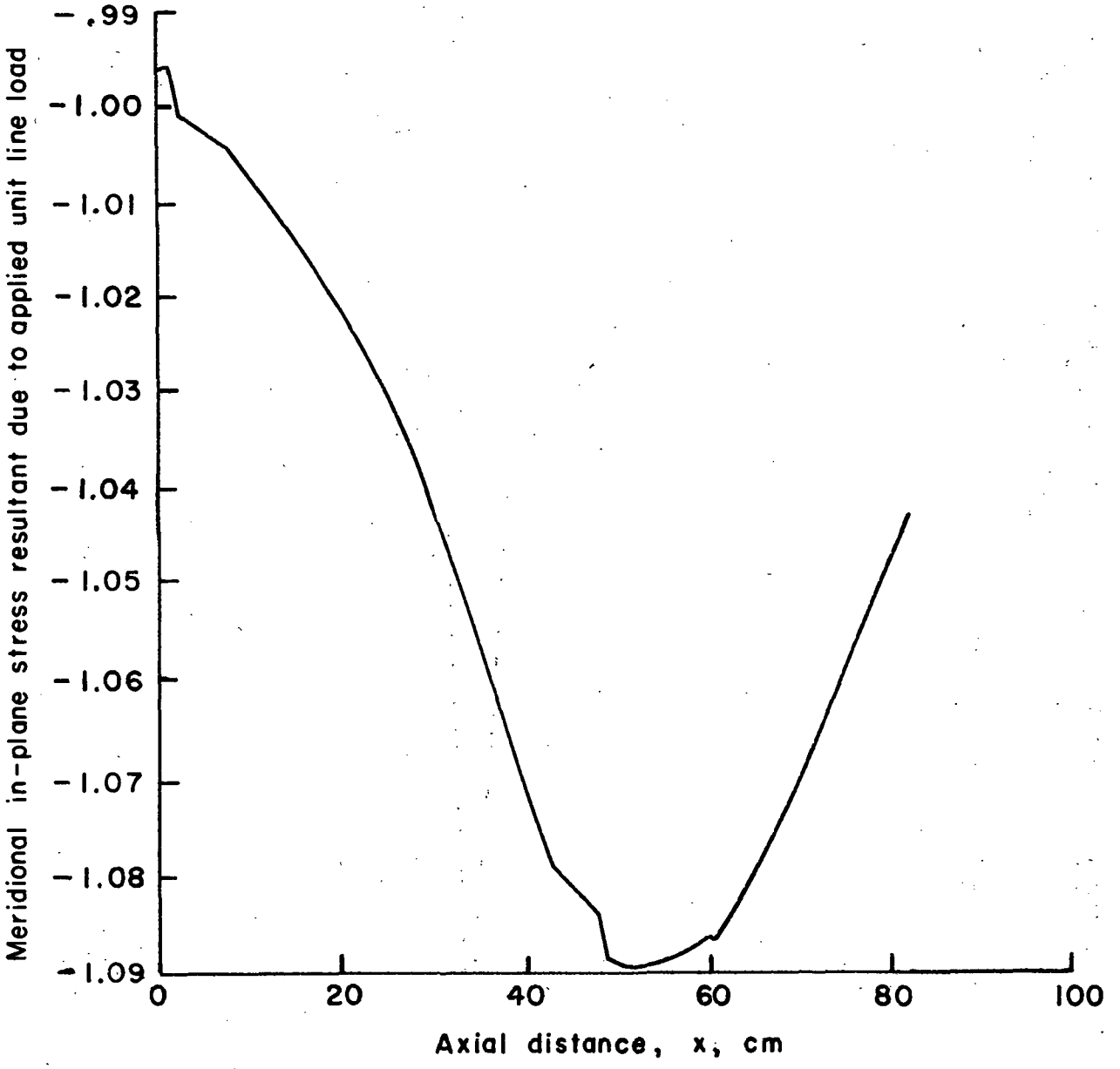

(b) $\theta = 70^{\circ}$.

Figure 6.- Continued.

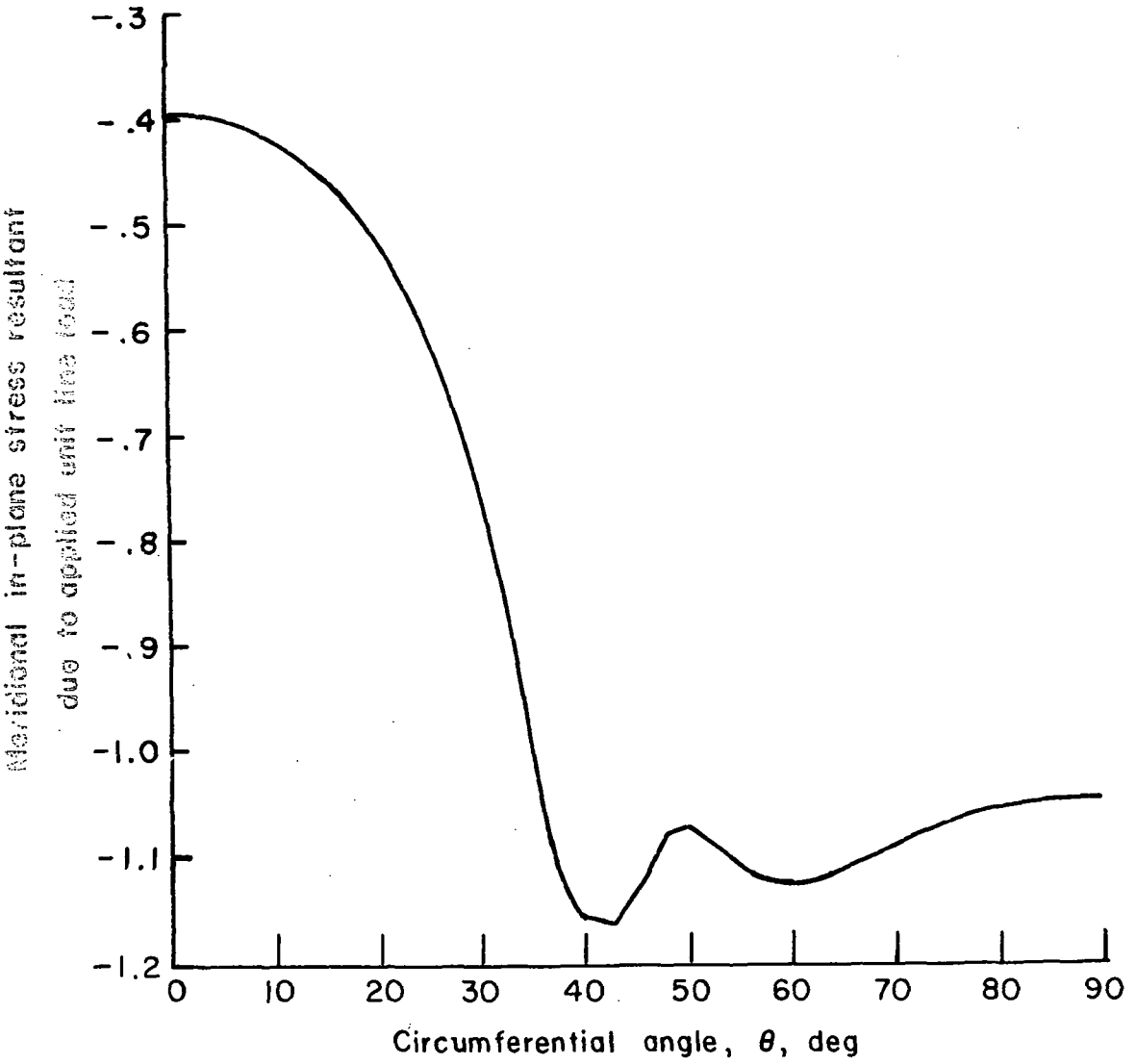

(c) x = 58.4 cm (lower edge of imperfection).

Figure 6.- Concluded.

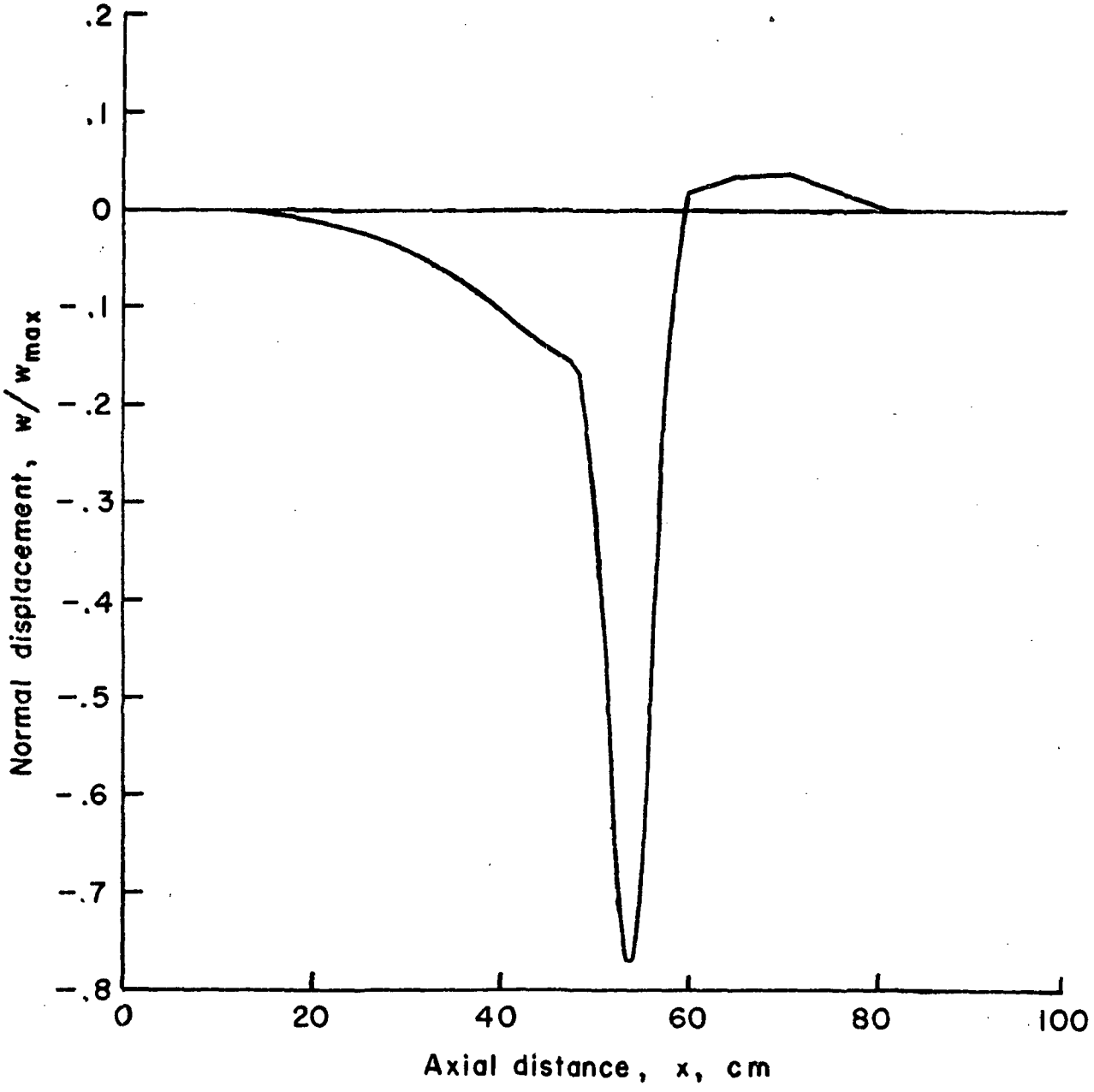

(a) $\theta = 41.1^{\circ}$.

Figure 7.- Normal displacement buckling mode for a cone with imperfection extending 90° along the circumference.

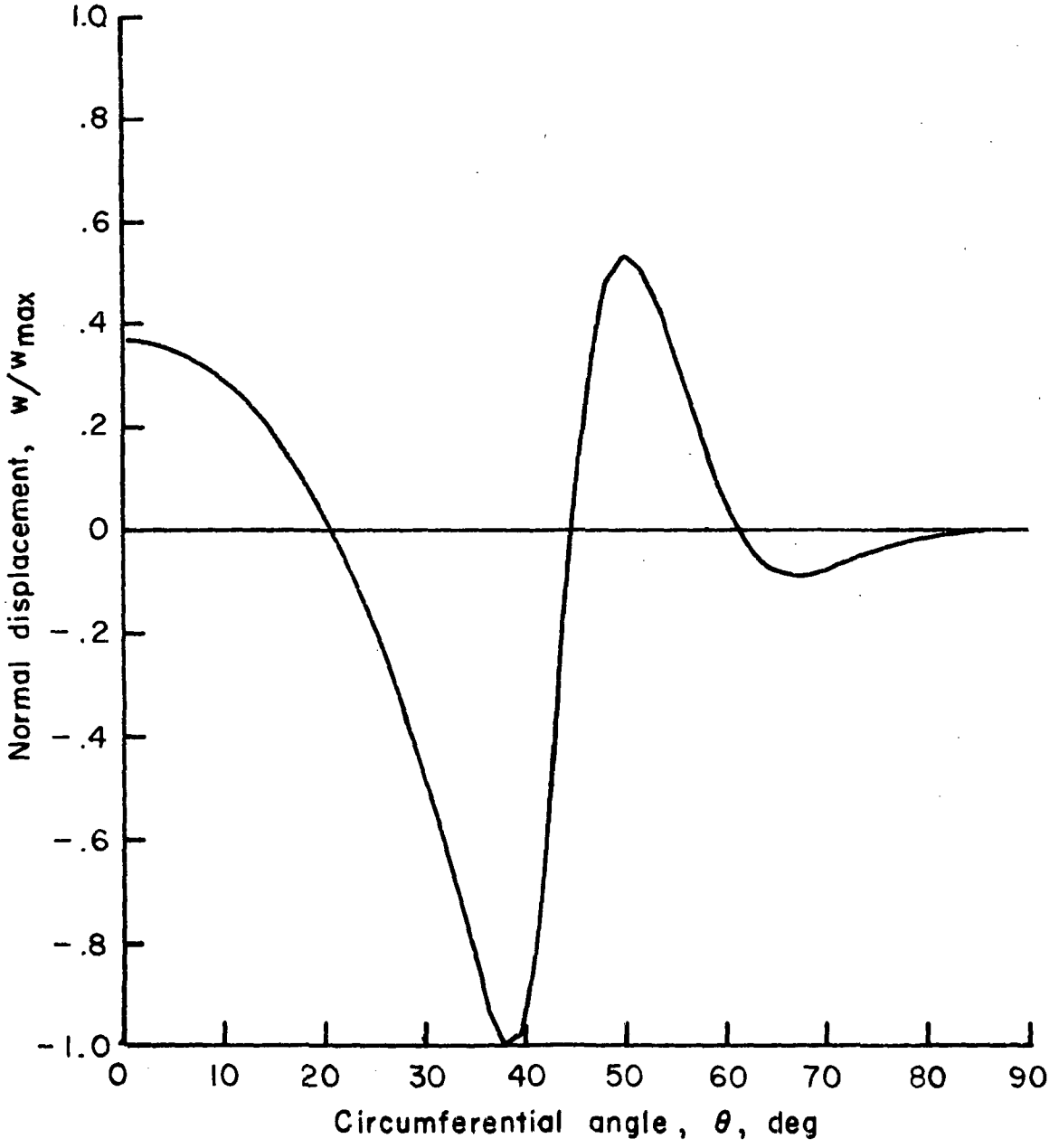

(b) x = 55.1 cm (near center of imperfection).

Figure 7.- Concluded.

NATIONAL AERONAUTICS AND SPACE ADMINISTRATION
WASHINGTON, D.C. 20546

OFFICIAL BUSINESS
PENALTY FOR PRIVATE USE $300

SPECIAL FOURTH-CLASS RATE BOOK

POSTAGE AND FEES PAID
NATIONAL AERONAUTICS AND SPACE ADMINISTRATION
451

U.S.MAIL

POSTMASTER: If Undeliverable (Section 158 Postal Manual) Do Not Return

"The aeronautical and space activities of the United States shall be conducted so as to contribute . . . to the expansion of human knowledge of phenomena in the atmosphere and space. The Administration shall provide for the widest practicable and appropriate dissemination of information concerning its activities and the results thereof."

—NATIONAL AERONAUTICS AND SPACE ACT OF 1958

NASA SCIENTIFIC AND TECHNICAL PUBLICATIONS

TECHNICAL REPORTS: Scientific and technical information considered important, complete, and a lasting contribution to existing knowledge.

TECHNICAL NOTES: Information less broad in scope but nevertheless of importance as a contribution to existing knowledge.

TECHNICAL MEMORANDUMS: Information receiving limited distribution because of preliminary data, security classification, or other reasons. Also includes conference proceedings with either limited or unlimited distribution.

CONTRACTOR REPORTS: Scientific and technical information generated under a NASA contract or grant and considered an important contribution to existing knowledge.

TECHNICAL TRANSLATIONS: Information published in a foreign language considered to merit NASA distribution in English.

SPECIAL PUBLICATIONS: Information derived from or of value to NASA activities. Publications include final reports of major projects, monographs, data compilations, handbooks, sourcebooks, and special bibliographies.

TECHNOLOGY UTILIZATION PUBLICATIONS: Information on technology used by NASA that may be of particular interest in commercial and other non-aerospace applications. Publications include Tech Briefs, Technology Utilization Reports and Technology Surveys.

Details on the availability of these publications may be obtained from:

SCIENTIFIC AND TECHNICAL INFORMATION OFFICE

NATIONAL AERONAUTICS AND SPACE ADMINISTRATION

Washington, D.C. 20546